ACS OMEGA

http://pubs.acs.org/journal/acsodf

Article

In Vivo Analgesic, Anti-Inflammatory, and Anti-Diabetic Screening of *Bacopa monnieri*-Synthesized Copper Oxide Nanoparticles

Shah Faisal,* Hasnain Jan, Abdullah, Ibrar Alam, Muhammad Rizwan, Zahid Hussain, Kishwar Sultana, Zafar Ali, and Muhammad Nazir Uddin

Cite This: *ACS Omega* 2022, 7, 4071−4082

Read Online

ACCESS | Metrics & More | Article Recommendations

ABSTRACT: In this work, an ecofriendly approach for biogenic production of copper oxide nanoparticles (CuO-NPs) was proposed by utilizing the *Bacopa monnieri* leaf extract as a reducing and stabilizing agent. The synthesis of CuO-NPs was instantly confirmed by a shift in the color of the copper solution from blue to dark gray. The use of UV−visible spectroscopy revealed a strong narrow peak at 535 nm, confirming the existence of monoclinic-shaped nanoparticles. The average size of CuO-NPs was 34.4 nm, according to scanning electron microscopy and transmission electron microscopy studies. The pristine crystalline nature of CuO-NPs was confirmed by X-ray diffraction. The monoclinic form of CuO-NPs with a crystallite size of 22 nm was determined by the sharp narrow peaks corresponding to 273, 541, 698, 684, and 366 Bragg's planes at different 2θ values. The presence of different reducing metabolites on the surface of CuO was shown by Fourier transform infrared analysis. The biological efficacy of CuO-NPs was tested against *Helicobacter felis*, *Helicobacter suis*, *Helicobacter salomonis.* and *Helicobacter bizzozeronii*. *H. suis* was the most susceptible strain with an inhibition zone of 15.84 ± 0.89 mm at 5 mg/mL of NPs, while the most tolerant strain was *H. bizzozeronii* with a 13.11 ± 0.83 mm of inhibition zone. In in vivo analgesic activity, CuO-NPs showed superior efficiency compared to controls. The maximum latency time observed was 7.14 ± 0.12 s at a dose level of 400 mg/kg after 90 min, followed by 5.21 ± 0.29 s at 400 mg/kg after 60 min, demonstrating 65 and 61% of analgesia, respectively. Diclofenac sodium was used as a standard with a latency time of 8.6 ± 0.23 s. The results observed in the rat paw edema assays showed a significant inhibitory activity of the plant-mediated CuO-NPs. The percentage inhibition of edema was 74% after 48 h for the group treated with CuO-NPs compared to the control group treated with diclofenac (100 mg/kg) with 24% edema inhibition. The solution of CuO-NPs produced 82% inhibition of edema after 21 days when compared with that of the standard drug diclofenac (73%). CuO-NPs vividly lowered glucose levels in STZ-induced diabetic mice, according to our findings. Blood glucose levels were reduced by about 33.66 and 32.19% in CuO-NP and (CuO-NP + insulin) groups of mice, respectively. From the abovementioned calculations, we can easily conclude that *B. monnieri*-synthesized CuO-NPs will be a potential antibacterial, anti-diabetic, and anti-inflammatory agent on in vivo and in vitro basis.

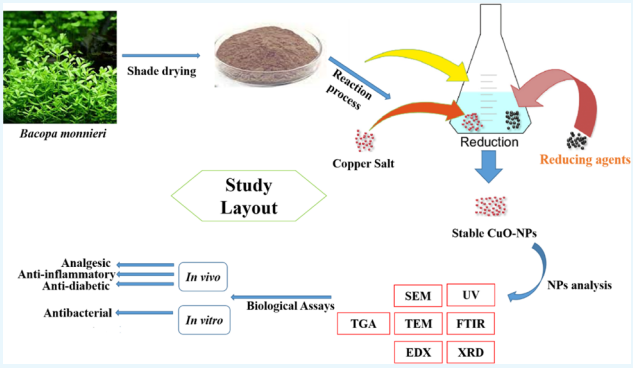

INTRODUCTION

Metal oxide nanoparticles (NPs) have sparked a lot of interest in optoelectronics, nanodevices, nanoelectronics, nanosensors, data storage, and catalysis in recent years.[1] Copper oxide nanoparticles (CuO-NPs), for example, are regarded as a strong weapon due to a wide range of advantageous properties, such as superconductivity at high temperatures, electron correlation effects, and spin dynamics.[2] Humans, plants, and animals all require copper (Cu). It is required by humans in trace amounts. Copper levels in the body of a 70 kg adult are around 100 mg. Copper consumption ranges from 2−4 mg per day, with a maximum of 10 mg.[3] The balance of the body's requirements must be met by dietary sources such as food or drink. Many enzymes, including those that are part of the human immune system's pathogen-killing machinery, require copper as a cofactor.[4] Many biochemical and physiochemical activities in plants require copper. It is one of the most important trace elements for plant development. A variety of enzymes, including amino oxidase, cytochrome c oxidase, and plastocyanin, use it as a cofactor.[5]

Received: September 29, 2021
Accepted: January 10, 2022
Published: January 27, 2022

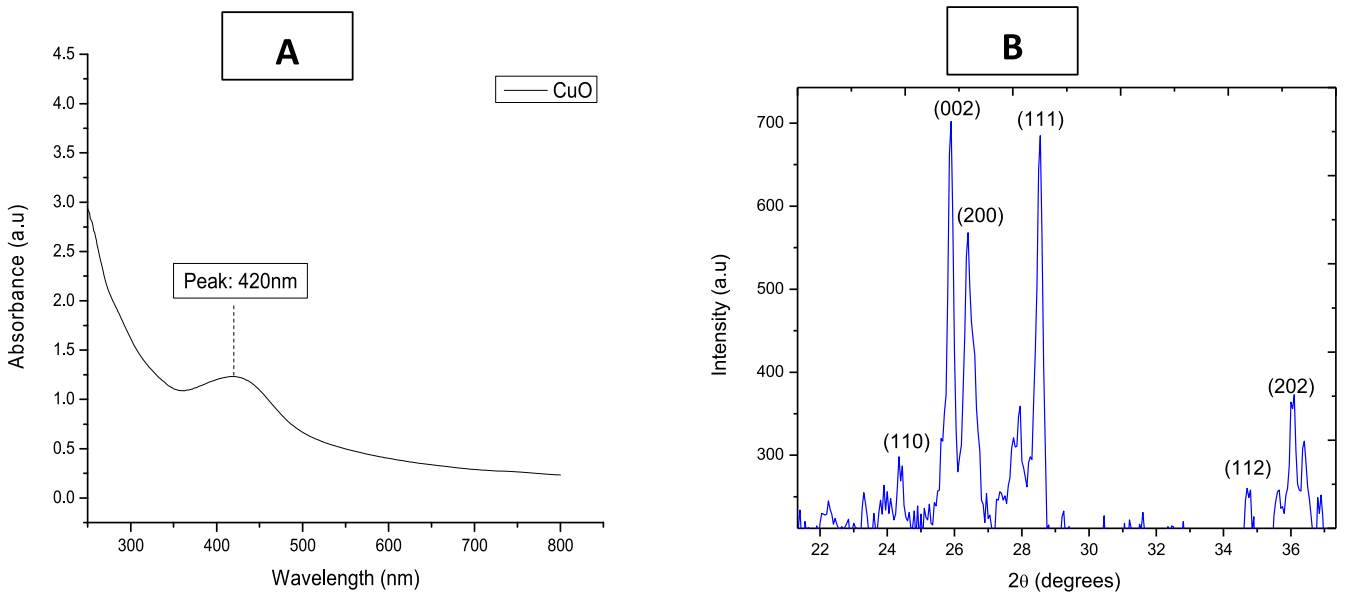

Figure 1. (A) UV-spectroscopic analysis and (B) typical XRD pattern of synthesized CuO-NPs.

People are interested in nanotechnology in the fields of physics, chemistry, biology, nanomedicine, and electronics as a result of the contemporary scientific period. Nanotechnology may create a wide range of nanoscale materials with at least one dimension, ranging in size from 1 to one 100 nm, known as nanomaterials or NPs.[6] Because of their capacity to be modified at a scale where characteristics can be controlled, nanomaterials have opened up new areas of scientific and industrial innovation. Due to the wide range of possible uses of NPs, a varied collection of researchers, including biologists, chemists, physicists, and engineers, took part.[7] These materials are used in sensors, textiles, batteries, nanomedicine, energy storage pigments, dyes, solar systems, capacitors, catalysis, food industries, lithium-ion batteries, plant metabolic pathways management, and wastewater treatment, to name a few.[8] Biological, chemical, and physical processes can be used to create NPs of various shapes and sizes.[9] Photochromic NPs, core−shell NPs, polymer-coated magnetite NPs, metal oxide NPs (including ZnO-NPs, MgO-NPs, FeO-NPs, and CuO-NPs), and metal dioxide NPs are just a few examples of NPs that can be classified based on their reported classification (TiO_2-NPs, CeO_2-NP, Ag-NPs, and ZrO_2-NPs).[10−13]

The prominence of CuO-NPs can be ascribed to their numerous uses. Copper oxide is a p-type semiconductor with a 1.7 eV band gap and a monoclinic crystal structure. CuO-NPs can be used for a variety of qualities and applications.[14] Copper oxide has a wide range of uses, including antimetastatic chemicals, antibacterials, antioxidants, drug delivery, anti-fungals, antibiotics, and anti-fouling.[15,16] A number of physicochemical methods were used to make CuO-NPs. Other disadvantages of these tactics include the release of several very harmful compounds into the environment as well as the significant financial and energy expense. As a result, a more environmentally friendly, green, and cost-effective method of producing NPs is required.[9] Biotechnology and other natural approaches, such as green chemistry, may be credited with the development of a cost-effective and environmentally friendly way for making NPs. Researchers used oleic acid, gelatin, albumin, starch, and alginate with fungus, algae, bacteria, plant extracts, and other living things to create CuO-NPs.[17] This approach is environmentally friendly, safe, and cost-effective, and it remains dynamic throughout.[18] Without various types of metabolites (proteins, enzymes, lipids, phenolic compounds, polysaccharides, and sugar) and functional groups such as metabolites, amino group, polyols, and carboxylic acid found in biotic resources, the reduction, chelation, stabilization, and production of NPs would be greatly hampered.[19]

Plant extracts are frequently employed to synthesize CuO-NPs. While the approach of fabricating CuO-NPs from bacteria, algae, and fungus has numerous benefits, it also has a few drawbacks.[9] Significant challenges, such as bacterial toxicity, the capacity to grow germs in isolation, and the incubation process, persist, however. Plant extracts are a fantastic source of antioxidants and a novel way to making NPs safer and more stable: manufacturing with plants is a quick and easy procedure that is also safer and more stable.[20] The procedure takes 1−3 h to finish at room temperature. Reduced and stabilizing agents, including phenols, flavonoids, tannins, terpenoids, and proteins, can be found among the bioactive metabolites in plant extracts. Electrons are created during the extraction of the plant, which causes copper salts to be decreased. Reducing molecules are formed when phytochemicals react with copper ions.[21,22]

In this study, we used the seed extract of *B. monnieri* as a reducing/capping agent to make CuO-NPs. It belongs to the Plantaginaceae family and is rich in phytochemicals such as bacoside saponins, known as dammarane types, with pseudo-jujubogenin as the aglycone moiety.[23,24] In the family, 12 bacoside analogues have been identified. Bacopasides I−XII are new saponins that have just been found. D-mannitol, apigenin, and herpestine B are among the five known alkaloids (herpestine, nicotine, brahmine, monnierasides I−III, and plantainoside B).[25] Apart from bacoside A, which was discovered to be a mixture of bacoside A3, bacopacide II, bacopasaponin C, and a jujubogenin isomer of bacosaponin C, the individual plant constituents that have received the most attention in this plant have been identified as bacoside A3, bacopacide II, bacopasaponin C, and jujubogenin.[26] *B. monnieri* has a number of scientific study uses, including

https://doi.org/10.1021/acsomega.1c05410
ACS Omega 2022, 7, 4071−4082

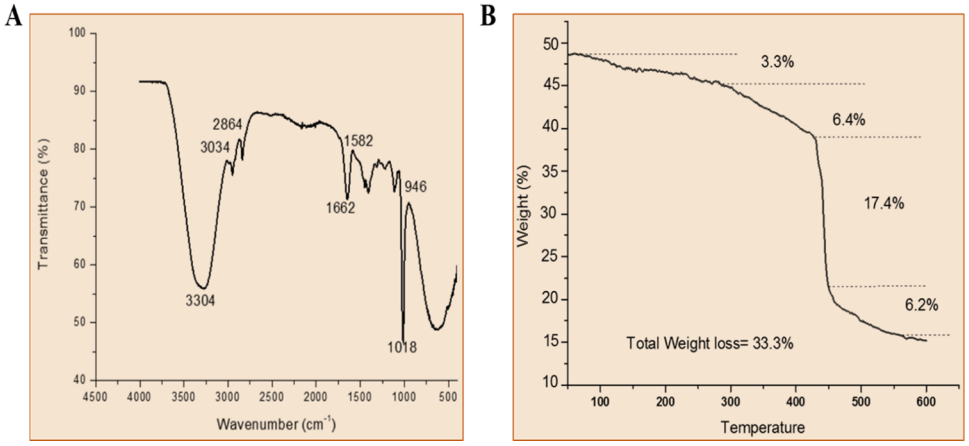

Figure 2. (A) FTIR analysis performed to find out available functional groups on the NP surface and (B) typical TGA graph of CuO-NPs.

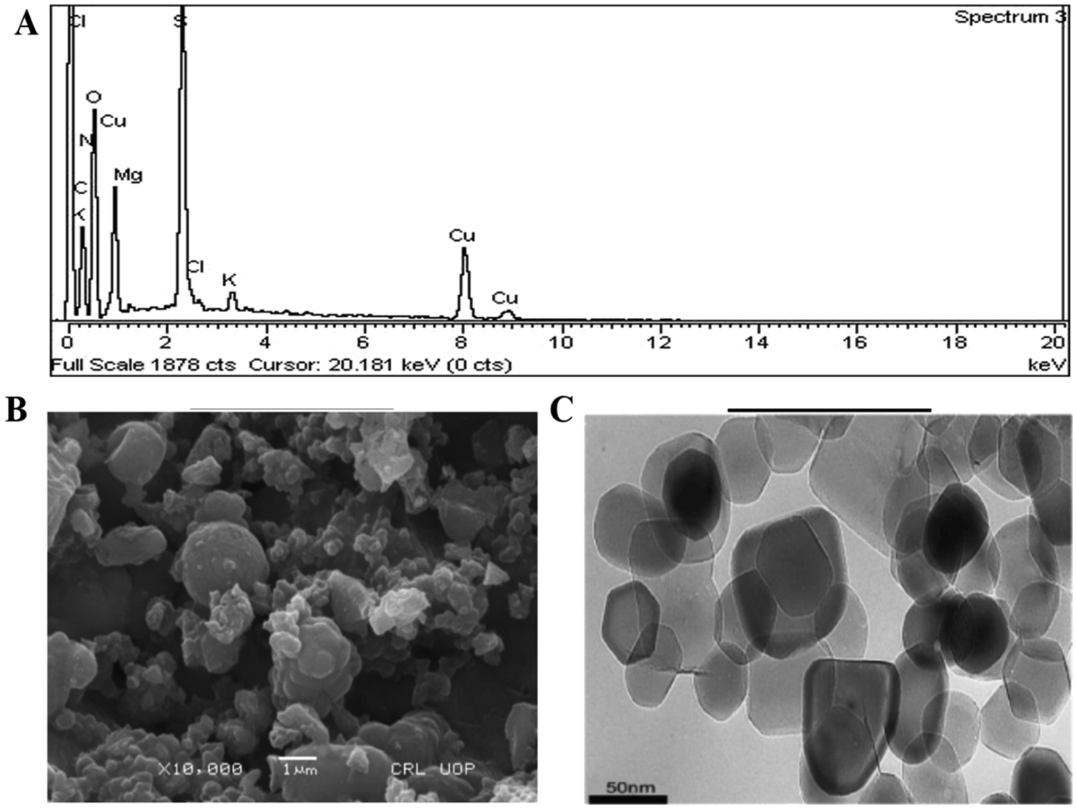

Figure 3. (A) EDX composition analysis, (B) SEM micrograph at 1 μm, and (C) TEM micrograph at 50 nm of CuO-NPs.

treating seizures, depression, pain, inflammation, ulcers, and liver health.[25] Fourier transform infrared (FTIR), ultra-violet (UV), X-ray diffraction (XRD), scanning electron microscopy (SEM), and transmission electron microscopy (TEM) were used to investigate the morphological and physicochemical properties of synthesized CuO-NPs. Finally, anti-arthritis, anti-diabetic, analgesic, leukocyte migration assay, and antibacterial assays were utilized to better assess the clinical effects of green CuO-NPs in order to find prospective pharmaceutical applications.

RESULTS AND DISCUSSION

Synthesis of Copper Nanoparticles. Seed extract of *B. monnieri* contains important phytochemicals such as bacoside A3, monnierasides I–III and saponins.[27,28] These phytochemicals have been used in the treatment of different diseases like pain and inflammation.[25] Aside from the biomedical importance, these phytochemicals can form strong bonds with metallic ions and is therefore a promising agent to be used in nanomaterial synthesis.[25,26] *B. monnieri* extract was used as a capping and reducing agent in the production of metallic NPs. When the reaction between *B. monnieri* and respective salts occurs, the color of the combination changes from dark blue to dark gray. For the investigation of its physico-chemical characteristics, the chemical was isolated and centrifuged before being stored.

UV Analysis. CuO-NPs were fabricated according to a well-established process, and the solution was kept at room temperature for 40 min after color change. The UV–visible spectral range was then set to 200–700 nm, and the sample

https://doi.org/10.1021/acsomega.1c05410
ACS Omega 2022, 7, 4071–4082

Table 1. Antibacterial Values of Synthesized CuO-NPs at Various Concentrations

	CuO-NPs			
H. pylori strains	5 mg/mL	4 mg/mL	2 mg/mL	1 mg/mL
Helicobacter felis	15.71 ± 0.91[a]	11.44 ± 1.13[a]	7.49 ± 0.67[b]	5.06 ± 0.55[b]
Helicobacter suis	15.84 ± 0.89[a]	11.26 ± 0.91[a]	8.39 ± 0.93[a]	4.86 ± 0.59[b]
Helicobacter salomonis	13.50 ± 0.84[b]	10.13 ± 0.73[b]	7.20 ± 0.84[b]	7.11 ± 0.59[a]
Helicobacter bizzozeronii	13.11 ± 0.83[c]	9.87 ± 0.78[c]	6.23 ± 0.81[c]	4.29 ± 0.44[c]
positive control (ampicillin)	23.82 ± 1.28	18.29 ± 1.12	14.67 ± 0.96	11.14 ± 0.88

[a]Highly significant. [b]Slightly significant. [c]Non-significant difference from control at $P < 0.05$ by one-way ANOVA in the column values are mean ± SD of triplicate.

was tested for absorbance.[29] This study was conducted using a Shimadzu UV-1800 Spectrophotometer. CuO-NPs were produced, as shown in Figure 1A, and validated by their distinctive surface plasmon peak at 420 nm at an absorbance rate of 1.25 a.u. A few tiny distortion peaks were also observed, which might be caused by proteins involved in NP reduction and capping.[30,31] The UV peaks successfully revealed that the Cu^{2+} ions were reduced to Cu^0 by *B. monnieri* macromolecules.

XRD Analysis. The phase identity and crystalline morphology of biosynthesized CuO-NPs were studied using an X-ray diffractometer (JDX-3532, JEOL, Japan) at 20−40 kV and 2.5−30 mA, respectively, using CuKa (wavelength = 1.5418) X-rays and a 2θ range of 0 to 160.[32] Figure 1B shows that the XRD main peaks at 110, 002, 200, 111, 112, and 202 correspond to 2θ values of 24.5, 25.8, 26.3, 28.7, 34.8, and 36.1°, respectively. As indicated by XRD data in Figure 1B, the CuO-NPs generated by the reduction of Cu^+ ions from the leaf extract are crystalline in nature. Before the XRD examination, the CuO-NPs were centrifuged many times and recollected in sterile distilled water, as stated above in the Biosynthesis of Copper Nanoparticles section, to eliminate any material that may ignite.[33] The appearance of structural peaks in XRD models indicates that the green synthesis of CuO-NPs is monoclinic space crystalline with an average crystal size of 22.4 nm.[33,34]

FTIR Analysis. The possible role of *B. monnieri* biomolecule functional groups in the capping and reduction of CuO-NPs was investigated using FTIR spectroscopy. The FTIR spectra were collected in the 400 to 4500 cm^{-1} spectral range using the Spectrum 3TM FTIR spectrometer.[35] Peaks were found at 3304, 3034, 2864, 1662, 1582, 1018, and 946 cm^{-1}, as shown in Figure 2A.[36] Stretching in aromatic CH_3 groups, C−H bond stretching in alkenes and alkanes, C═C bond stretching in alkenes, N−O bond stretching in nitro compounds,[37] O−H bond stretching in carboxylic acid, and C═C bond bending in alkenes are all involved in the reduction of Cu^{+2}.

Thermal Galvanometric Analysis. Pyris Diamond Series thermal galvanometric analysis (TGA) was utilized to investigate the thermal properties of CuO-NPs between 50 and 600 °C, as illustrated in Figure 2B. CuO-NPs lost 33.3% of their total weight when heated to 600 °C. The first weight loss occurred at a temperature of roughly 150 °C owing to dehydration and moisture loss.[38] While the rate of weight loss increased as the temperature rose, the amount of weight lost at 400 °C was minimal.

Energy Dispersive X-Ray Analysis. Energy dispersive X-ray (EDX) using (JSM5910) INCA200/Oxford instruments, UK, was accomplished in the voltage range of 0−20 KeV. The EDX technique may be used to determine the elemental analysis of biosynthesized NPs.[39] According to the EDX spectra displayed in Figure 3A, there is a prominent peak of copper at 0.3 KeV as well as two additional peaks at 8.0 and 8.41 KeV. Additional K, Cl, S, O, Mg, and C peaks were also found, which might be related to biomolecules participating in NP production. The existence of copper NPs was confirmed by the high peaks of copper.[40] The new peaks had no effect on the copper NPs' real nanostructure.

SEM and TEM Morphological Analysis. The precise shape and size of the biosynthesized CuO-NPs were determined using SEM and TEM.[41] The analysis was carried out using a scanning electron microscope (JSM5910) and transmission electron microscope (JEM-2100). With an average size of 34.4 nm, the white patches in Figure 3B represent particle agglomeration, with some particles uniformed and monodispersed and others aggregated and polydispersed (ImageJ analysis). Figure 3C displays a TEM microphotograph of copper oxide, which reveals its monoclinic structure. The aggregation of the particles is caused by the fast reduction of biomolecules during the creation of CuO-NPs. The size of the particles is, however, affected by the salt content and the pH of the reaction. In comparison to low pH, high pH causes greater aggregation and bigger size.[42]

Antibacterial Assay. One of the most serious issues in global health care is the development of antibiotic resistance in bacterial strains. Metal NPs and their oxides are one of the most promising approaches to combat antibiotic resistance in bacteria. Numerous investigations have demonstrated that metal oxide NPs have a strong antibacterial capability against both Gram-positive and Gram-negative bacterial species.[43] The utilization of metal-based NPs and their oxides is of particular interest. Copper (Cu) and its oxides (CuO) are one of the most researched metals that impact living things. Copper is a very active element with excellent reduction characteristics. Copper oxide is easily formed when it is oxidized. Copper is one of the most significant trace elements in the human body.[44] Most metals, such as copper, zinc, and iron, exert their antimicrobial effects by inhibiting enzymes, causing the formation of reactive oxygen species (ROS) (the Fenton reaction), damaging cell membranes, and preventing microorganisms from obtaining critically essential microelements.[45] When metal oxide NPs interact with bacteria, they produce ROS. Metal ions produced by NPs have an impact on the respiratory chain and block certain enzymes. Singlet oxygen, hydroxyl radical, hydrogen peroxide, superoxide anions, and other ROS are formed and accumulate as a result. Bacterial internal components such as DNA and proteins can be damaged by ROS.[46] This antibacterial activity is shown in Table 1 and Figure 4 using the disk diffusion method, which uses CuO-NPs. Four pathogenic bacteria strains, namely, *Helicobacter felis*, *Helicobacter suis*, *Helicobacter salomonis*, and *Helicobacter bizzozeronii*, were evaluated against various concentrations of NPs ranging from 5 to 0.5 mg/mL. In

https://doi.org/10.1021/acsomega.1c05410
ACS Omega 2022, 7, 4071−4082

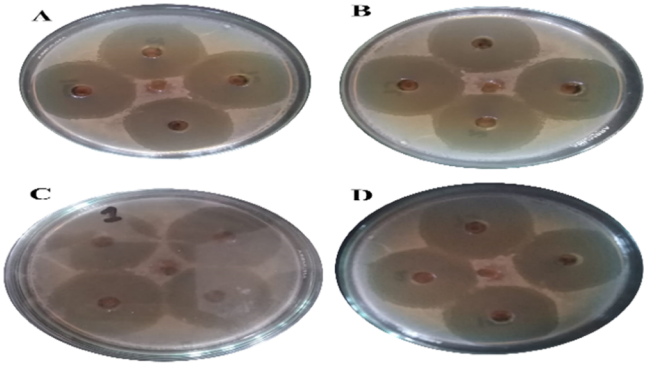

Figure 4. Assay picture of NPs against various strains of *H. pylori:* (A) *H. felis*, (B) *H. salomonis*, (C) *H. suis*, and (D) *H. bizzozeronii*.

these activities, ampicillin was employed as a positive control. A tested bacterial strain had its highest bactericidal activity against CuO-NPs that were added to the medium at a concentration of 5 mg/mL. At a high concentration, the CuO-NPs were shown to be bactericidal, while at a lower concentration, they were shown to be bacteriostatic. *H. salomonis*, *H. felis*, *H. suis*, and *H. bizzozeronii* all showed strong inhibition zones of 13.50 ± 0.84, 15.71 ± 0.91, 15.84 ± 0.89, and 13.11 ± 0.83, respectively, against 5 mg/mL. Biofabricated CuO-NPs have gained interest as an antibacterial therapy due to their unique morphologies, diameters, and biocompatibility. A type of CuO-NPs is antimicrobial, working against both Gram-positive and Gram-negative bacteria.[47,48] Previous studies have shown that the antibacterial property of CuO-NPs is produced through a green method utilizing the *Tabernaemontana divaricata* leaf extract and shown against *Helicobacter pylori*.[49]

Analgesic Activity. Controlling pain is a significant goal in the treatment of many disorders. Using a hot plate approach, many synthetic compounds and metallic NPs are investigated for pain-relieving properties in Swiss albino mice.[50] To locate a bioactive molecule, natural commodities are required, particularly from medicinal plants with little or no side effects.[50,51] The mean delay time (seconds) was measured after the injection of prepared CuO-NPs (30, 60, and 90 min). Group I (which had a mean delay time of 2.37 ± 0.11 s after 30 min of saline administration) experienced a significantly long latency time of 8.6 ± 0.23 s after receiving diclofenac sodium; this was compared to the control group (which had a mean delay time of 2.37 ± 0.11 s after 30 min of saline administration). CuO-NPs showed a significant and dose-dependent analgesic impact in contrast to the control condition. After 90 min, a maximum mean latency time of 7.14 s was recorded at a dosage level of 400 mg/kg, which reduced to 5.21 s at the same dose level after 60 min, suggesting pain alleviation of 65 and 61%, respectively. Figures 5 and 6 demonstrate that 8.6 ± 0.23 s had to elapse after diclofenac sodium was administered in order to create a standard. Flavonoid-rich plants have been found to have analgesic, diuretic, and anti-inflammatory properties. *B. monnieri* leaf extracts also include flavonoids and phenols, which help in the formation of CuO-NPs.[52,53]

In vivo Anti-Inflammatory Assay. *Reduction of Carrageenan-Induced Paw Edema in Rats.* In the pharmaceutical research, the rat paw inflammation caused by the chemical carrageenan is widely used to aid in the search for new anti-inflammatory medications.[54] Carrageenan injection

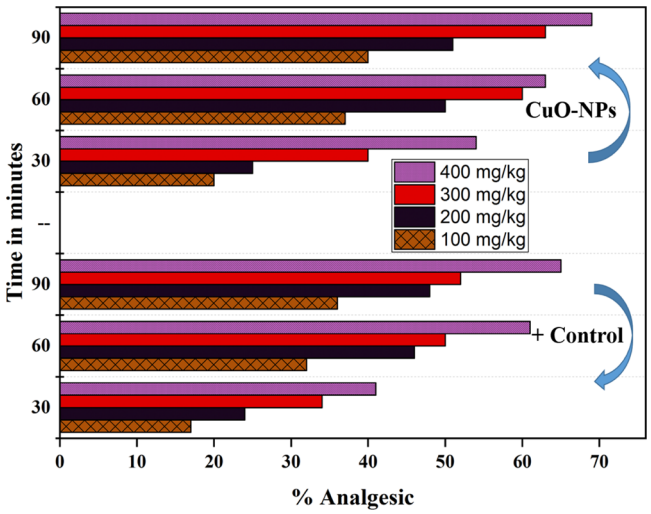

Figure 5. Percentage analgesic potential of synthesized CuO-NPs.

induces a rise in histamine-, serotonin-, and prostaglandin-like substances in the rat's paw, resulting in edema development.[55] The anti-inflammatory properties of CuO-NPs are anticipated to be substantial because they block histamine, serotonin, and prostaglandin.[56] According to the current data, NPs are a useful therapeutic agent for decreasing inflammation in acute situations (see Table 2 and Figure 7). Plant-mediated CuO-NPs often show a substantial inhibition efficacy in rat paw edema experiments. After 48 h, the CuO-NP-treated group had 74% less edema than the diclofenac (100 mg/kg)-treated control group. Post 48 h, the CuO-NP group showed a 74% reduction in edema as compared to the diclofenac (100 mg/kg)-treated control group. The findings confirmed that the number of white blood cells traveling to the location of inflammation had increased. In this test model, prostaglandins were found to be involved in the inflammatory process. Edema in the paw is caused by inflammatory mediators that increase vascular permeability and/or mediators that increase blood flow.[57,58]

Leukocyte Migration. The number of leukocytes attracted to the air-induced cavity after the carrageenan injection alone was 6×10^5 cells/mL higher than the number of leukocytes found in the group treated with the anti-inflammatory drug diclofenac (4.5×10^5 cells/mL) or in the group treated with the NPs (3.5×10^5 cells/mL), as shown in Figure 8.[59,60]

Reduction of Adjuvant Arthritis-Induced Paw Edema. Pre-injection of CuO-NPs revealed that compared to the control group, it was possible to reduce paw edema in rats by administering the treatment for a total of 21 days. CuO-NPs yielded an 82% reduction in edema after 21 days, as indicated in Table 3 and Figure 9. In the current research, the CuO-NPs, as opposed to the conventional medication, were shown to be effective in reducing the complete Freund's adjuvant (CFA)-induced chronic inflammation in the rat knee joint. The CuO-NPs studied in the CFA-induced monoarthritis resulted in substantially decreased paw volume in comparison to the control.[61] Phenolic and terpenoid chemicals are known to possess anti-inflammatory properties, and this may explain the anti-inflammatory effects in these experiences.[62] Based on findings obtained via the leukocyte migration test, it seems that the mechanism of action of NPs involves altering the migration of leukocytes into the tissues and target organs.[63] Adjuvant arthritis is utilized widely in etiology research as well as to

https://doi.org/10.1021/acsomega.1c05410
ACS Omega 2022, 7, 4071−4082

Figure 6. Analgesic activity of CuO-NPs.

Table 2. Effect of CuO-NPs in Carrageenan-Induced Rat Hind Paw Edema

treatments and doses	0 h	1 h	2 h	3 h	4 h	5 h	24 h	48 h
carrageenan 1% percentage of inhibition	0	0	0	0	0	0	0	0
Diclofenac 100 mg/mL percentage of inhibition	0	48	39	36	49	47	34	24
NPs 400 mg/mL percentage of inhibition	0	45	49	57	58	60	66	74

evaluate novel natural treatments. In the rat adjuvant arthritis model, several herbal remedies have been shown to lessen the extent of the illness. Antioxidant activity has also been said to have a role in the reduction of inflammation and arthritic processes.[64]

In Vivo Anti-Diabetic Assay. Many metallic NPs, such as zinc, silver, iron, copper, and gold oxides, have been employed in medical and biological sciences.[65] This work reveals that injecting CuO-based NPs into diabetic mice leads to considerable blood glucose reductions even when the mice are not fasting, as shown in Tables 4 and 5. Hepatic glycogenolysis and gluconeogenesis contribute to hyperglycemia by promoting excessive synthesis of glucose and discouraging its use by the tissues.[66] We found that CuO-NPs decreased the levels of glucose in STZ-induced diabetic mice substantially. When compared with the control group, about 35.74 and 32.78% reductions in blood glucose levels were observed for the groups of mice treated with CuO-NPs and (CuO-NPs + insulin), respectively. The drug STZ enters the β-cell via a glucose transporter and damages the DNA with alkylation.[67] Poly-ADP-ribosylation is a mechanism that is much more essential for the diabetes-inducing capability of STZ than DNA damage itself. Zinc may help promote the actions of insulin and may decrease the formation of cytokines, which has the potential to kill the insulin-secreting cells in the pancreas, causing type 1 diabetes.[68]

Biocompatibility with Human Red Blood Cells. It was discovered that learning about the adverse effects of CuO-NPs on human exposure could be done by measuring the percentage of human blood impacted by high concentrations of CuO-NPs (CuO-NPs at concentrations ranging from 400 to 12.5 μg/mL). Human red blood cells were extracted from the circulatory system and used in a study to see if they were biocompatible when combined with CuO-NPs.[69] The cytotoxic nature of these generated CuO-NPs at the highest concentration was shown by the percentage of CuO-NPs that were hemolyzed, as indicated in Table 6; that is, at 400 μg/mL the percentage was 4.54 $\pm$ 0.31 and at 12.5 μg/mL the percentage was 2.36 $\pm$ 0.24. It was discovered that the hemolysis efficacy of CuO-NPs decreases as the CuO-NP concentration is lowered. Our research revealed that the safe concentration of CuO-NPs was 12.5 μg/mL, and hemolysis potential was related to the size of the NPs.[70]

CONCLUSIONS

The formation of CuO-NPs by eco-friendly and green bioprinting with *B. monnieri* leaf extract was demonstrated in the current work. The CuO-NPs were analyzed using a variety of analytical methods, including UV, XRD, FTIR, SEM, TEM, and EDX. In vitro and in vivo studies have demonstrated that

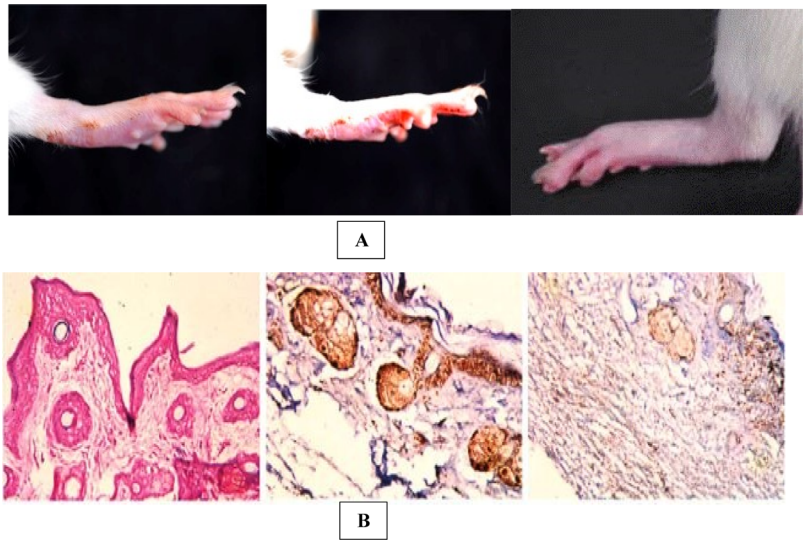

Figure 7. Reduction of carrageenan-induced paw edema in rats. (A) Picture of paw. (B) Histopathology of paw edema.

https://doi.org/10.1021/acsomega.1c05410
ACS Omega 2022, 7, 4071−4082

Figure 8. Leukocyte migration assay of CuO-NPs.

Table 3. Reduction of Adjuvant Arthritis-Induced Paw Edema

DAY February	CFA + DICLOF 10 mg/kg % inhibition	CFA + NPs 400 mg/kg % inhibition
February 1	10	12
February 3	18	21
February 6	29	32
February 9	36	41
February 12	45	49
February 15	58	61
February 18	67	71
February 21	73	82

Table 4. Anti-Diabetic Effect of CuO-NPs on STZ-Induced Diabetic Mice

groups	dose	fasting blood glucose levels (mmol/L)	glucose levels after 2 h	% of inhibition
control distal water	1 mL/mice (oral)	17.59 ± 0.43	17.54 ± 0.18	
NPs	14 mg/kg bw (oral)	17.19 ± 0.32	10.13 ± 0.29	35.74
NPs + insulin	7 mg/kg bw (oral) + 0.2 U/50 g (sc)	17.59 ± 0.39	10.52 ± 0.33	32.78
G-IV (standard: insulin)	0.4 U/50 g (sc)	17.68 ± 0.44	8.41 ± 0.27	43.60

this CuO-NP formulation possesses antibacterial, anti-diabetic, and anti-inflammatory activities. CuO-NPs showed a strong antimicrobial and anti-diabetic activity as a result of the findings, which might lead to the development of novel antibacterial and anti-diabetic medications. However, this study looked at the molecular processes and physiological aspects of CuO-NPs; further research is needed to understand the link between these mechanisms and the clinical consequences observed in mice. The introduction of phytoconstituents that are both active and have higher characteristics has boosted the biological uses of CuO-NPs. As a result, *B. monnieri* seed extract might be an effective alternative to traditional treatments.

METHODS

Herb Collection and Extract Preparation. Disease-free and healthy *B. monnieri* leaves were collected from Charsadda, KPK, Pakistan. The Department of Botany, Bacha Khan University, Pakistan, was cited as the taxonomic authority after obtaining confirmation that the plant had been identified as *B. monnieri*. To eliminate pollutants and dust spores, the plant material was gently rinsed with distilled water. After 40 days of drying in the shade, the leaves were finely powdered in a grinder. A mixture of 10 g finely powdered leaves and 100 mL

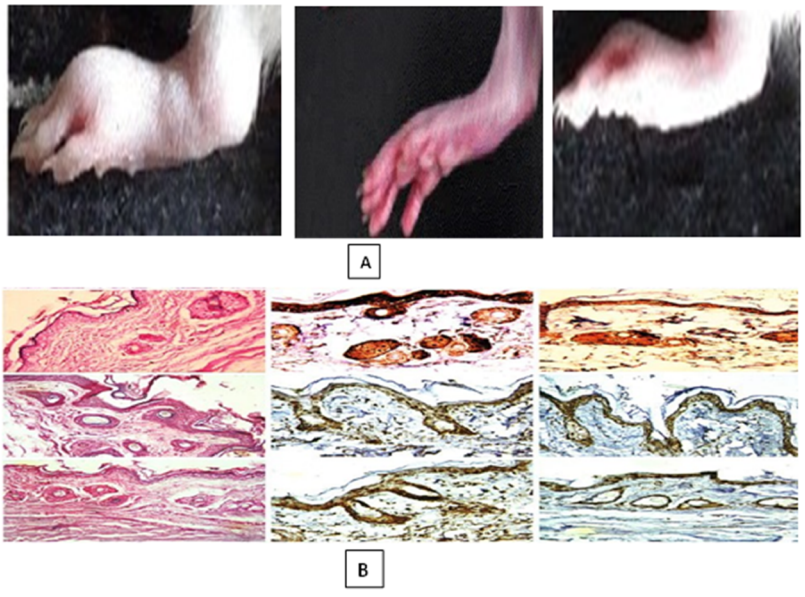

Figure 9. Reduction of adjuvant arthritis-induced paw edema in rats. (A) Picture of a rat knee joint. (B) Histopathology of rat knee joint tissues.

https://doi.org/10.1021/acsomega.1c05410
ACS Omega 2022, 7, 4071−4082

Table 5. Hypoglycemic Activity of CuO-NPs

groups	dose	blood glucose levels (mmol/L) fasting glucose levels	glucose levels after 2 h	% of inhibition
control distal water	1 mL/mice (oral)	5.10 ± 0.12	4.98 ± 0.06	
NPs, mild dose	8 mg/kg bw (oral)	4.71 ± 0.22	3.75 ± 0.23	23.19
NPs, moderate dose	14 mg/kg bw (oral)	5.29 ± 0.29	3.66 ± 0.19	27.17
standard: glibenclamide	10 mg/kg bw (oral)	5.07 ± 0.18	3.19 ± 0.21	44.31

Table 6. Biocompatible Nature of CuO-NPs against hRBCs

S. no	concentration (μg/mL)	% hemolysis
1	400	4.54 ± 0.31
2	200	4.28 ± 0.33
3	100	3.63 ± 0.30
4	50	2.74 ± 0.30
5	25	2.61 ± 0.29
6	12.5	2.36 ± 0.24

distilled water was mixed for 1 h at 60 °C. The extract was first filtered through two layers of nylon filter paper and then purified three times with Whatman filter paper no. 1. After filtering the copper sulfate, the liquid was allowed to cool before being blended with the copper salt. The extract was kept at 4 °C until it was tested.[71]

Synthesis of CuO-NPs. A previously disclosed technique for making copper oxide NPs was revised to add new aspects.[32] To conduct a sensitivity experiment, 100 mL of the extract was mixed with 6.0 g of cupric acetate $Cu(CH_3COO)_2$ (Sigma-Aldrich) and heated to 60 °C for 2 h on a magnetic stirrer. The solution was chilled to 25 °C before centrifuging (at 10,000 rpm for 10 min). The resulting pellet was washed three times with purified water before being put onto a clean Petri dish and dried in the oven at 90 °C. After smashing the material into a fine powder with a pestle and mortar, it was exposed to 2 h treatment at 500 °C to remove any impurities.

Physicochemical and Morphological Characterization. UV−vis spectroscopy, XRD, FTIR, SEM, TEM, and TG testing were employed to investigate the structural, vibrational, chemical, and morphological properties of biosynthesized CuO-NPs. The model D8 Advance XRD (Germany) was used to determine the crystallinity of the material, in the temperature range of $2v$ (10−80°) with a scanning step size of 0.03°/s. The use of Cu K radiation was necessary in order to get diffraction data (wavelength 1.5406, generator voltage 40 kV, tube current 30 mA). Using Scherer's equation, the crystallite size was calculated as follows:[72]

$$D = k\lambda/\beta \cos\theta$$

EDX analysis was used to test the chemical composition of synthesized NPs. As a consequence of capping and reducing agents within the extract, FTIR analysis identified functional groups on NPs. This experiment was done in distilled water with varying pH values in order to visually evaluate particle scattering stability. The structure/appearance and morphology of the NPs was measured via SEM. To evaluate the size and shape of biogenic CuO-NPs, TEM was used.[73]

Antibacterial Activity of CuO-NPs against *H. pylori* Bacterial Strains. The bactericidal potential of CuO-NPs in solution was investigated in vitro utilizing the agar well diffusion technique with minimal modifications.[74] The seeding density of the bacterial culture (1 × 106 CFU/mL) was modified to reach the highest effective seeding density. The nutrient agar lawn was created with 50 μL of newly cultured microorganisms. A test sample of 10 μL was placed in each well. The seeded plates were then labeled in the same way. The names were also spelled out on the seeded plates. As a positive control, ampicillin was utilized, while DMSO was used as a negative control. After a 24 h incubation period at 37 °C, the zone of inhibition was measured in all of the test wells that included samples and controls. The breadth of the zones was measured using a Vernier Caliper's millimeter gauge.

Analgesic Activity of CuO-NPs. Albino mice were given for this study by the National Institute of Health in Islamabad, Pakistan. The mice were housed at a temperature of 25 °C with a relative humidity of 50−55% and given 12 h cycles of light and darkness to keep the temperatures in the colony cages under control. The animals were given typical animal feed to eat. The animals were housed in a facility that offered a constant and controlled setting to begin the experiment. While the standard procedure was followed, the hot plate method was applied to boost analgesic effect. The feet of mice are extremely temperature sensitive. They elevate their paws and escape when they detect a temperature shift. The mice were kept on Eddy's hot plate at 54.2 °C. A 15 s protective time was observed in order to prevent paw skin harm. A timer was used to measure the time it took for a mouse to respond. Diclofenac sodium was used as a positive control to confirm the findings. Intraperitoneal injections of CuO-NPs at concentrations of 100, 200, 300, and 400 mg/kg were used. After 30, 60, and 90 min, three mice were given NPs of varying concentrations and monitored.

Carrageenan-Induced Paw Edema in Rats. Rats in the test group showed edema in their right hind paws after being injected with 0.2 mL of 1% (w/v) carrageenan (Sigma-Aldrich, St. Louis, USA), with a volume of 0.2 mL, on the plantar side of the right hind paw.[75] Before the carrageenan injection, the paw diameter was measured. After the carrageenan injection, the paw diameter was measured each hour up to five times, then after 24 and 48 h. The rats were split into three groups, where each group included six members. For the first group (control group), normal saline was administered (3 mL/kg body weight), whereas for the second group, the usual anti-inflammatory medication was used; diclofenac (Troge, Germany) (100 mg/kg body weight p.o.) was given. The NPs (400 mg/kg body weight po) were given to the third group. One hour before administering carrageenan, the animals were pretreated. Using this method, we estimated the percentage inhibition of edema

$$\%\ \text{inhibition of edema} = \frac{\text{Mean edema increase in control group} - \text{Mean edema increase in treated group}}{\text{Mean edema increase in control group}} \times 100$$

https://doi.org/10.1021/acsomega.1c05410
ACS Omega 2022, 7, 4071−4082

Adjuvant-Induced Chronic Arthritis. Injecting CFA into the left footpad of each rat caused experimental arthritis in that animal (CFA, Difco Laboratories, Detroit, MI, USA). The NPs (500 mg/kg body weight po) were given to the rats daily for 21 days following the CFA challenge, as was done in the test groups. To keep it clear, in the third group, the drug diclofenac (10 mg/kg body weight po) was administered, while in the control group, a saline solution (3 mL/kg body weight po) was administered.

Leukocyte Migration Assay. Dorsal subcutaneous air pouches (20 mL sterile air) were created in four groups of rats as reported before carrageenan (1%) was injected into the created cavity of three groups and 0.9% NaCl was put into one group on the third day after the cavity was established. A 4-day treatment of the test sample (500 mg/kg body weight po) following the air pouches therapy was given to the rats in the test groups. In the control group, saline was given to those receiving it (3 mL/kg body weight). In the third group, diclofenac was administered to those receiving it (100 mg/kg body weight). The leukocyte count was assessed after 5 mL of ice-cold 0.9% NaCl was injected into the cavity and subsequently collected.[75]

Induction of Experimental Diabetes. Experimental mice were injected intraperitoneally (ip) with STZ (45 mg/kg body weight) to develop diabetes. For 5 consecutive days, mice were injected with STZ dissolved in freshly produced 0.01 M sodium citrate buffer (pH = 4.5), and their blood was collected. To minimize the risk of hypoglycemia after STZ injection, the animals were made to consume glucose solution (5% w/v) overnight.[76] Mice in the control group simply received the vehicle (citrate buffer). STZ-treated mice were allowed to stay in their usual environment for 5 days after the treatment was finished. Mice who had been on the diet for about 2 weeks following the 2-week fasting period acquired diabetes and had blood glucose levels of >11.1 mmol/L while they were fasting. In order to determine blood glucose levels, the STZ-treated mice were tethered for 12 h and blood samples were taken from the tail vein. Mice with blood glucose levels more than 11.1 mmol/L after fasting were identified as having diabetes, and therefore, they were chosen for further research.

Animal Grouping. For the anti-diabetic activity test, diabetic mice were divided into four groups, each with five mice. Mice were organized into two groups, G and I, with only distilled water being administered to both groups[77] The results of these experiments may be broken down into four groups. These are referred to as the standard treatment group, where diabetic mice were injected with 0.4 units insulin subcutaneously (per 50 mg of body weight) [G-II (CuO-NP treated), G-III (CuO-NP and insulin treated), and G-IV]. Each group received their respective doses over 14 consecutive days. A total of 20 mice were selected and divided into four groups. Then, the research proceeded according to a well-established procedure[78] Three separate experiments were run to study the effect of groups (G-I, G-II, and G-IV) on mice. An oral glucose tolerance test has the following interpretation: 6 h after fasting, mice were given 2 g of glucose per kilogram of body weight. Then, before the CuO-NP dosage, they were given glucose by mouth. Blood glucose was tested at 0, 15, 30, 60, and 90 min after being inserted into the bloodstream. The control group had distilled water (1 mL/mouse, oral); the second group had CuO-NPs (8 mg/kg body weight, oral); the third group had CuO-NPs (14 mg/kg body weight, oral); and the fourth group had glibenclamide (10 mg/kg body weight, oral).[79]

Biochemical Determination. Blood glucose levels were measured using the "ACCU-CHEK Active" kit glucose oxidase technique. Before starting the experimental procedures, the animals' blood glucose levels were tested. Fasting blood glucose levels were monitored regularly until diabetes was discovered.

Sampling Protocol. All of the animals included in the experiment had 2−3 L of blood drawn from their tail veins. The ACCU-CHEK active blood glucose meter was used to monitor the blood glucose levels.

Biocompatibility Assay. Fresh hRBCs were used to demonstrate the biocompatibility of biogenic CuO-NPs.[80] After the individual's permission, 1 mL blood samples were obtained in EDTA tubes from healthy persons. Following the collection, the blood samples were centrifuged to isolate RBCs. Following centrifugation, a supernatant and pellet were produced; the supernatant was discarded, and the pellet was collected after three washes with PBS. PBS-erythrocyte suspension was made by combining 200 L of RBCs with 9.8 mL of PBS (pH 7.2). The erythrocyte suspension and green produced CuO-NPs were then combined in Eppendorf tubes. After that, the Eppendorf tubes containing the erythrocyte suspension and NPs were incubated for 1 h at 35 °C. The reaction mixture was centrifuged at 12,000 rpm for 10 min before transferring 200 L of the supernatant to a 96-well plate and recording hemoglobin release absorption spectra at 450 nm. The formula for calculating percent hemolysis was

$$''(\%)\text{hemolysis} = \left(\frac{\text{sample Ab} - \text{negative control Ab}}{\text{positive control Ab} - \text{negative control Ab}}\right) \times 100'$$

where Ab denotes the reported absorbance of the samples.

AUTHOR INFORMATION

Corresponding Author

Shah Faisal − *Institute of Biotechnology and Microbiology, Bacha Khan University, Charsadda 24460 KPK, Pakistan;* orcid.org/0000-0001-5474-2622; Email: shahfaisal11495@gmail.com

Authors

Hasnain Jan − *Institute of Biochemical Sciences, National Taiwan University, Taipei City 10617, Taiwan;* orcid.org/0000-0002-7225-2595

Abdullah − *Department of Microbiology, Abdul Wali Khan University, Mardan 23200 KPK, Pakistan*

Ibrar Alam − *Nanoscience and Nanotechnology, Faculty of Science, King Mongkut's University of Technology, Thonburi, Bangkok 10140, Thailand*

Muhammad Rizwan − *Center for Biotechnology and Microbiology University of Swat, Khyber Pakhtunkhwa 44000, Pakistan*

Zahid Hussain − *Center for Biotechnology and Microbiology University of Swat, Khyber Pakhtunkhwa 44000, Pakistan*

Kishwar Sultana − *Center for Biotechnology and Microbiology University of Peshawar, Peshawar 25000 KPK, Pakistan*

Zafar Ali − *Center for Biotechnology and Microbiology University of Swat, Khyber Pakhtunkhwa 44000, Pakistan*

https://doi.org/10.1021/acsomega.1c05410
ACS Omega 2022, 7, 4071−4082

Muhammad Nazir Uddin − *Center for Biotechnology and Microbiology University of Swat, Khyber Pakhtunkhwa 44000, Pakistan*

Complete contact information is available at: https://pubs.acs.org/10.1021/acsomega.1c05410

Author Contributions

Shah Faisal: Concept, idea, investigation, manuscript writing. Hasnain Jan: review and software. Abdullah: software, characteriazation analysis and edit. Ibrar Alam: software and revesion. Muhammad Rizwan, Zahid Hussain, Kishwar Sultana, Zafar Ali, and Muhammad Nazir Uddin: revesion and edit of manuscript.

Funding

No fund was taken from any source.

Notes

The authors declare no competing financial interest.

■ ACKNOWLEDGMENTS

We are thankful to all the institutions associated with authors for providing resources.

■ REFERENCES

(1) Madkour, L. H. *Nanoelectronic Materials: Fundamentals and Applications*; Springer, 2019; Vol. *116*.

(2) Stockman, M. I.; Kneipp, K.; Bozhevolnyi, S. I.; Saha, S.; Dutta, A.; Ndukaife, J.; Kinsey, N.; Reddy, H.; Guler, U.; Shalaev, V. M.; Boltasseva, A.; Gholipour, B.; Krishnamoorthy, H. N. S.; MacDonald, K. F.; Soci, C.; Zheludev, N. I.; Savinov, V.; Singh, R.; Groß, P.; Lienau, C.; Vadai, M.; Solomon, M. L.; Barton, D. R.; Lawrence, M.; Dionne, J. A.; Boriskina, S. V.; Esteban, R.; Aizpurua, J.; Zhang, X.; Yang, S.; Wang, D.; Wang, W.; Odom, T. W.; Accanto, N.; de Roque, P. M.; Hancu, I. M.; Piatkowski, L.; van Hulst, N. F.; Kling, M. F. Roadmap on plasmonics. *J. Opt.* **2018**, *20*, 043001.

(3) Xiong, T.; Dumat, C.; Dappe, V.; Vezin, H.; Schreck, E.; Shahid, M.; Pierart, A.; Sobanska, S. Copper oxide nanoparticle foliar uptake, phytotoxicity, and consequences for sustainable urban agriculture. *Environ. Sci. Technol.* **2017**, *51*, 5242−5251.

(4) Zhang, S.; Liu, H.; Amarsingh, G. V.; Cheung, C. C. H.; Wu, D.; Narayanan, U.; Zhang, L.; Cooper, G. J. S. Restoration of myocellular copper-trafficking proteins and mitochondrial copper enzymes repairs cardiac function in rats with diabetes-evoked heart failure. *Metallomics* **2020**, *12*, 259−272.

(5) Shabbir, Z.; Sardar, A.; Shabbir, A.; Abbas, G.; Shamshad, S.; Khalid, S.; Natasha, G.; Murtaza, G.; Dumat, C.; Shahid, M. Copper uptake, essentiality, toxicity, detoxification and risk assessment in soil-plant environment. *Chemosphere* **2020**, *259*, 127436.

(6) Kargozar, S.; Mozafari, M. Nanotechnology and Nanomedicine: Start small, think big. *Mater. Today: Proc.* **2018**, *5*, 15492−15500.

(7) Noreen, S.; Tahir, M. B.; Hussain, A.; Nawaz, T.; Rehman, J. U.; Dahshan, A.; Alzaid, M.; Alrobei, H. Emerging 2D-Nanostructured materials for electrochemical and sensing Application-A review. *Int. J. Hydrogen Energy* **2022**, *47*, 1371.

(8) Waris, A.; Din, M.; Ali, A.; Afridi, S.; Baset, A.; Khan, A. U.; Ali, M. Green fabrication of Co and Co3O4 nanoparticles and their biomedical applications: A review. *Open Life Sci.* **2021**, *16*, 14−30.

(9) Salem, S. S.; Fouda, A. Green synthesis of metallic nanoparticles and their prospective biotechnological applications: an overview. *Biol. Trace Elem. Res.* **2021**, *199*, 344−370.

(10) Popov, A. L.; Zholobak, N. M.; Balko, O. I.; Balko, O. B.; Shcherbakov, A. B.; Popova, N. R.; Ivanova, O. S.; Baranchikov, A. E.; Ivanov, V. K. Photo-induced toxicity of tungsten oxide photochromic nanoparticles. *J. Photochem. Photobiol., B* **2018**, *178*, 395−403.

(11) Esquivel-Castro, T. A.; Ibarra-Alonso, M. C.; Oliva, J.; Martínez-Luévanos, A. Porous aerogel and core/shell nanoparticles for controlled drug delivery: a review. *Mater. Sci. Eng., C* **2019**, *96*, 915−940.

(12) Wallyn, J.; Anton, N.; Vandamme, T. F. Synthesis, Principles, and Properties of Magnetite Nanoparticles for In Vivo Imaging Applications-A Review. *Pharmaceutics* **2019**, *11*, 601.

(13) Nikam, A. V.; Prasad, B. L. V.; Kulkarni, A. A. Wet chemical synthesis of metal oxide nanoparticles: a review. *CrystEngComm* **2018**, *20*, 5091−5107.

(14) Waris, A.; Din, M.; Ali, A.; Ali, M.; Afridi, S.; Baset, A.; Khan, A. U. A comprehensive review of green synthesis of copper oxide nanoparticles and their diverse biomedical applications. *Inorg. Chem. Commun.* **2021**, *123*, 108369.

(15) Javed, R.; Rais, F.; Kaleem, M.; Jamil, B.; Ahmad, M. A.; Yu, T.; Qureshi, S. W.; Ao, Q. Chitosan capping of CuO nanoparticles: Facile chemical preparation, biological analysis, and applications in dentistry. *Int. J. Biol. Macromol.* **2021**, *167*, 1452−1467.

(16) Abd, A. N.; Hassoni, M. H.; Hasan, M. H. Properties and biomedical applications of copper oxide nanoparticles. *Biochem. Cell. Arch.* **2018**, *18*, 1763−1766.

(17) Verma, M. L.; Dhanya, B. S.; Sukriti, V.; Rani, V.; Thakur, M.; Jeslin, J.; Kushwaha, R. Carbohydrate and protein based biopolymeric nanoparticles: current status and biotechnological applications. *Int. J. Biol. Macromol.* **2020**, *154*, 390−412.

(18) Sanjini, N. S.; Winston, B.; Velmathi, S. Effect of precursors on the synthesis of CuO nanoparticles under microwave for photocatalytic activity towards methylene blue and rhodamine B dyes. *J. Nanosci. Nanotechnol.* **2017**, *17*, 495−501.

(19) Ovais, M.; Khalil, A. T.; Islam, N. U.; Ahmad, I.; Ayaz, M.; Saravanan, M.; Shinwari, Z. K.; Mukherjee, S. Role of plant phytochemicals and microbial enzymes in biosynthesis of metallic nanoparticles. *Appl. Microbiol. Biotechnol.* **2018**, *102*, 6799−6814.

(20) Saratale, R. G.; Karuppusamy, I.; Saratale, G. D.; Pugazhendhi, A.; Kumar, G.; Park, Y.; Ghodake, G. S.; Bharagava, R. N.; Banu, J. R.; Shin, H. S. A comprehensive review on green nanomaterials using biological systems: Recent perception and their future applications. *Colloids Surf., B* **2018**, *170*, 20−35.

(21) Zikalala, N.; Matshetshe, K.; Parani, S.; Oluwafemi, O. S. Biosynthesis protocols for colloidal metal oxide nanoparticles. *Nano-Struct. Nano-Objects* **2018**, *16*, 288−299.

(22) Aboyewa, J. A.; Sibuyi, N. R. S.; Meyer, M.; Oguntibeju, O. O. Green synthesis of metallic nanoparticles using some selected medicinal plants from southern africa and their biological applications. *Plants* **2021**, *10*, 1929.

(23) Joshi, T.; Gupta, A.; Kumar, P.; Singh, A.; Kumar, A. *Bacopa monnieri (Brahmi). In Naturally Occurring Chemicals Against Alzheimer's Disease*; Elsevier, 2021; pp 243−256.

(24) Choudhary, S.; Kumari, I.; Thakur, S.; Kaurav, H.; Chaudhary, G. BRAHMI (BACOPA MONNIERI)−A POTENTIAL AYURVEDIC COGNITIVE ENHANCER AND NEUROPROTECTIVE HERB. *Int. J. Ayurveda Pharma Res.* **2021**, 41−49.

(25) Banerjee, S.; Anand, U.; Ghosh, S.; Ray, D.; Ray, P.; Nandy, S.; Deshmukh, G. D.; Tripathi, V.; Dey, A. Bacosides from Bacopa monnieri extract: An overview of the effects on neurological disorders. *Phytother. Res.* **2021**, *35*, 5668.

(26) Ritter, S.; Urmann, C.; Herzog, R.; Glaser, J.; Bieringer, S.; Geisberger, T.; Eisenreich, W.; Riepl, H. Where is Bacosine in commercially available Bacopa monnieri? *Planta Med.* **2020**, *86*, 565−570.

(27) Dutta, S.; Chakraborty, S. Estimation of phytochemical characteristics and antioxidant property of secondary metabolites of a memory enhancing medicinal herb Baccopa monnieri of East Kolkata Wetland. *Int. J. Pharm. Sci. Res.* **2020**, *11*, 2860−2867.

(28) Rai, K.; Gupta, N.; Dharamdasani, L.; Nair, P.; Bodhankar, P. Bacopa monnieri: a wonder drug changing fortune of people. *Int. J. Appl. Sci. Biotechnol.* **2017**, *5*, 127−132.

(29) Hasanin, M.; Hashem, A. H.; Lashin, I.; Hassan, S. A. In vitro improvement and rooting of banana plantlets using antifungal nanocomposite based on myco-synthesized copper oxide nanoparticles and starch. *Biomass Convers. Biorefin.* **2021**, 1−11.

(30) Bouafia, A.; Laouini, S. E.; Ouahrani, M. R. A review on green synthesis of CuO nanoparticles using plant extract and evaluation of antimicrobial activity. *Asian J. Res. Chem.* **2020**, *13*, 65−70.
(31) Gu, H.; Chen, X.; Chen, F.; Zhou, X.; Parsaee, Z. Ultrasound-assisted biosynthesis of CuO-NPs using brown alga Cystoseira trinodis: Characterization, photocatalytic AOP, DPPH scavenging and antibacterial investigations. *Ultrason. Sonochem.* **2018**, *41*, 109−119.
(32) Faisal, S.; Al-Radadi, N. S.; Jan, H.; Abdullah, S. A.; Shah, S. A.; Shah, S.; Rizwan, M.; Afsheen, Z.; Hussain, Z.; Uddin, M. N.; Idrees, M.; Bibi, N. Curcuma longa Mediated Synthesis of Copper Oxide, Nickel Oxide and Cu-Ni Bimetallic Hybrid Nanoparticles: Characterization and Evaluation for Antimicrobial, Anti-Parasitic and Cytotoxic Potentials. *Coatings* **2021**, *11*, 849.
(33) Aziz, W. J.; Abid, M. A.; Hussein, E. H. Biosynthesis of CuO nanoparticles and synergistic antibacterial activity using mint leaf extract. *Mater. Technol.* **2020**, *35*, 447−451.
(34) Mohamed, H. E. A.; Thema, T.; Dhlamini, M. S. Green synthesis of CuO nanoparticles via Hyphaene thebaica extract and their optical properties. *Mater. Today: Proc.* **2021**, *36*, 591−594.
(35) Faisal, S.; Jan, H.; Shah, S. A.; Shah, S.; Khan, A.; Akbar, M. T.; Rizwan, M.; Jan, F.; Wajidullah; Akhtar, N.; Khattak, A.; Syed, S. Green synthesis of zinc oxide (ZnO) nanoparticles using aqueous fruit extracts of Myristica fragrans: their characterizations and biological and environmental applications. *ACS Omega* **2021**, *6*, 9709−9722.
(36) Parsaee, Z.; Karachi, N.; Razavi, R. Ultrasound assisted fabrication of a novel optode base on a triazine based Schiff base immobilized on TEOS for copper detection. *Ultrason. Sonochem.* **2018**, *47*, 36−46.
(37) Rakhimol, K. R.; Thomas, S.; Kalarikkal, N.; Jayachandran, K. Casein mediated synthesis of stabilized metal/metal-oxide nanoparticles with varied surface morphology through pH alteration. *Mater. Chem. Phys.* **2020**, *246*, 122803.
(38) Ismail, M.; Gul, S.; Khan, M. I.; Khan, M. A.; Asiri, A. M.; Khan, S. B. Green synthesis of zerovalent copper nanoparticles for efficient reduction of toxic azo dyes congo red and methyl orange. *Green Process. Synth.* **2019**, *8*, 135−143.
(39) Sebeia, N.; Jabli, M.; Ghith, A. Biological synthesis of copper nanoparticles, using Nerium oleander leaves extract: characterization and study of their interaction with organic dyes. *Inorg. Chem. Commun.* **2019**, *105*, 36−46.
(40) Sebeia, N.; Jabli, M.; Ghith, A.; Saleh, T. A. Eco-friendly synthesis of Cynomorium coccineum extract for controlled production of copper nanoparticles for sorption of methylene blue dye. *Arabian J. Chem.* **2020**, *13*, 4263−4274.
(41) Rajeshkumar, S.; Rinitha, G. Nanostructural characterization of antimicrobial and antioxidant copper nanoparticles synthesized using novel Persea americana seeds. *OpenNano* **2018**, *3*, 18−27.
(42) Sun, H.; Jiao, R.; Xu, H.; An, G.; Wang, D. The influence of particle size and concentration combined with pH on coagulation mechanisms. *J. Environ. Sci.* **2019**, *82*, 39−46.
(43) Shah, M.; Nawaz, S.; Jan, H.; Uddin, N.; Ali, A.; Anjum, S.; Giglioli-Guivarc'h, N.; Hano, C.; Abbasi, B. H. Synthesis of bio-mediated silver nanoparticles from Silybum marianum and their biological and clinical activities. *Mater. Sci. Eng., C* **2020**, *112*, 110889.
(44) Jiang, Q.; Zhu, Y. F.; Zhao, M. Copper metallization for current very large scale integration. *Recent Pat. Nanotechnol.* **2011**, *5*, 106−137.
(45) Gudkov, S. V.; Burmistrov, D. E.; Serov, D. A.; Rebezov, M. B.; Semenova, A. A.; Lisitsyn, A. B. A Mini Review of Antibacterial properties of ZnO nanoparticles. *Front. Phys.* **2021**, *9*, 641481.
(46) Vatansever, F.; de Melo, W. C. M. A.; Avci, P.; Vecchio, D.; Sadasivam, M.; Gupta, A.; Chandran, R.; Karimi, M.; Parizotto, N. A.; Yin, R.; Tegos, G. P.; Hamblin, M. R. Antimicrobial strategies centered around reactive oxygen species - bactericidal antibiotics, photodynamic therapy, and beyond. *FEMS Microbiol. Rev.* **2013**, *37*, 955−989.
(47) Kotrange, H.; Najda, A.; Bains, A.; Gruszecki, R.; Chawla, P.; Tosif, M. M. Metal and Metal Oxide Nanoparticle as a Novel Antibiotic Carrier for the Direct Delivery of Antibiotics. *Int. J. Mol. Sci.* **2021**, *22*, 9596.
(48) Ren, G.; Hu, D.; Cheng, E. W. C.; Vargas-Reus, M. A.; Reip, P.; Allaker, R. P. Characterisation of copper oxide nanoparticles for antimicrobial applications. *Int. J. Antimicrob. Agents* **2009**, *33*, 587−590.
(49) Sivaraj, R.; Rahman, P. K. S. M.; Rajiv, P.; Salam, H. A.; Venckatesh, R. Biogenic copper oxide nanoparticles synthesis using Tabernaemontana divaricate leaf extract and its antibacterial activity against urinary tract pathogen. *Spectrochim. Acta, Part A* **2014**, *133*, 178−181.
(50) Chiguvare, H.; Oyedeji, O.; Matewu, R.; Aremu, O.; Oyemitan, I.; Oyedeji, A.; Nkeh-Chungag, B.; Songca, S.; Mohan, S.; Oluwafemi, O. Synthesis of silver nanoparticles using Buchu plant extracts and their analgesic properties. *Molecules* **2016**, *21*, 774.
(51) Shah, S.; Shah, S. A.; Faisal, S.; Khan, A.; Ullah, R.; Ali, N.; Bilal, M. Engineering novel gold nanoparticles using Sageretia thea leaf extract and evaluation of their biological activities. *J. Nanostruct. Chem.* **2021**, 1−12.
(52) Kim, S.; Ryu, D.-Y. Silver nanoparticle-induced oxidative stress, genotoxicity and apoptosis in cultured cells and animal tissues. *J. Appl. Toxicol.* **2013**, *33*, 78−89.
(53) Shah, S.; Siraj-ud-Din, R. Pharmacognostic standardization and FT-IR analysis of various parts of Sageretia thea. *Int. J. Biosci.* **2013**, *3*, 108−114.
(54) Ravi, V.; Mohamed Saleem, T.; Patel, S.; Raamamurthy, J.; Gauthaman, K. Anti-inflammatory effect of methanolic extract of Solanum nigrum Linn berries. *Int. J. Appl. Res. Nat. Prod.* **2009**, *2*, 33−36.
(55) Halici, Z.; Dengiz, G. O.; Odabasoglu, F.; Suleyman, H.; Cadirci, E.; Halici, M. Amiodarone has anti-inflammatory and anti-oxidative properties: an experimental study in rats with carrageenan-induced paw edema. *Eur. J. Pharmacol.* **2007**, *566*, 215−221.
(56) Simak, J. The effects of engineered nanomaterials on cultured endothelial cells. *HANDBOOK OF IMMUNOLOGICAL PROPERTIES OF ENGINEERED NANOMATERIALS: Volume 2: Haemato-compatibility of Engineered Nanomaterials*; World Scientific, 2016; pp 105−162.
(57) Subhan, F.; Karim, N.; Ibrar, M. Anti-inflammatory activity of methanolic and aqueous extracts of Valeriana wallichii DC rhizome. *Pak. J. Plant Sci.* **2007**, *13*, 103−108.
(58) Zhang, Z.; Chinnathambi, A.; Ali Alharbi, S.; Bai, L. Copper oxide nanoparticles from Rabdosia rubescens attenuates the complete Freund's adjuvant (CFA) induced rheumatoid arthritis in rats via suppressing the inflammatory proteins COX-2/PGE2. *Arabian J. Chem.* **2020**, *13*, 5639−5650.
(59) AbouAitah, K.; Higazy, I. M.; Swiderska-Sroda, A.; Abdelhameed, R. M.; Gierlotka, S.; Mohamed, T. A.; Szałaj, U.; Lojkowski, W. Anti-inflammatory and antioxidant effects of nano-formulations composed of metal-organic frameworks delivering rutin and/or piperine natural agents. *Drug Delivery* **2021**, *28*, 1478−1495.
(60) Badawy, A. M. Review article on Chemical constituents and Biological activity of Thymelaea hirsuta. *Rec. Pharm. Biomed. Sci.* **2019**, *3*, 28−32.
(61) Tseuguem, P. P.; Ngangoum, D. A. M.; Pouadjeu, J. M.; Piégang, B. N.; Sando, Z.; Kolber, B. J.; Tidgewell, K. J.; Nguelefack, T. B. Aqueous and methanol extracts of Paullinia pinnata L. (Sapindaceae) improve inflammation, pain and histological features in CFA-induced mono-arthritis: Evidence from in vivo and in vitro studies. *J. Ethnopharmacol.* **2019**, *236*, 183−195.
(62) Belemlilga, M. B.; Traoré, T. K.; Boly, G. A. L.; Ouédraogo, N.; Traoré, A.; Lompo, M.; Ouédraogo, S.; Pierre Guissou, I. Evaluation of Antioxidant, Anti-inflammatory and Analgesic Activities of Leaves of Saba senegalensis (A.DC) Pichon (Apocynaceae). *Eur. J. Med. Plants* **2019**, 1−12.
(63) Dudics, S.; Langan, D.; Meka, R.; Venkatesha, S.; Berman, B.; Che, C.-T.; Moudgil, K. Natural products for the treatment of autoimmune arthritis: their mechanisms of action, targeted delivery,

https://doi.org/10.1021/acsomega.1c05410
ACS Omega 2022, 7, 4071−4082

and interplay with the host microbiome. *Int. J. Mol. Sci.* **2018**, *19*, 2508.
(64) Govindarajan, S.; Babu, S. N.; Noor, A. Evaluation of In Vitro and In Vivo Anti-oxidant and Anti-inflammatory Potential of Aloe vera Gel Extract. *Phytomedicine*; CRC Press, 2020; pp 145−155. DOI: 10.1201/9781003014898-15
(65) Madkour, L. H. Ecofriendly green biosynthesized of metallic nanoparticles: bio-reduction mechanism, characterization and pharmaceutical applications in biotechnology industry. *Global Drugs Ther.* **2017**, 3. DOI: 10.15761/GDT.1000144.
(66) Rendell, M. S. Current and emerging gluconeogenesis inhibitors for the treatment of Type 2 diabetes. *Expert Opin. Pharmacother.* **2021**, *22*, 2167−2179.
(67) Pansare, K.; Upasani, C.; Upangalwar, A.; Sonawane, G.; Patil, C. STREPTOZOTOCIN AND ALLOXAN INDUCED DIABETIC NEPHROPATHY: PROTECTIVE ROLE OF NATURAL PRODUCTS. *J. Maharaja Sayajirao Univer. Baroda* **2021**, *55*, 86.
(68) Bjørklund, G.; Dadar, M.; Pivina, L.; Doşa, M. D.; Semenova, Y.; Aaseth, J. The role of zinc and copper in insulin resistance and diabetes mellitus. *Curr. Med. Chem.* **2020**, *27*, 6643−6657.
(69) Khalil, A. T.; Ovais, M.; Ullah, I.; Ali, M.; Shinwari, Z. K.; Maaza, M. Physical properties, biological applications and biocompatibility studies on biosynthesized single phase cobalt oxide (Co3O4) nanoparticles via Sageretia thea (Osbeck.). *Arabian J. Chem.* **2020**, *13*, 606−619.
(70) Ansari, S. M.; Bhor, R. D.; Pai, K. R.; Sen, D.; Mazumder, S.; Ghosh, K.; Kolekar, Y. D.; Ramana, C. V. Cobalt nanoparticles for biomedical applications: Facile synthesis, physiochemical characterization, cytotoxicity behavior and biocompatibility. *Appl. Surf. Sci.* **2017**, *414*, 171−187.
(71) Jan, H.; Zaman, G.; Usman, H.; Ansir, R.; Drouet, S.; Gigliolo-Guivarc'h, N.; Hano, C.; Abbasi, B. H. Biogenically proficient synthesis and characterization of silver nanoparticles (Ag-NPs) employing aqueous extract of Aquilegia pubiflora along with their in vitro antimicrobial, anti-cancer and other biological applications. *J. Mater. Res. Technol.* **2021**, *15*, 950−968.
(72) Jan, H.; Shah, M.; Usman, H.; Khan, M. A.; Zia, M.; Hano, C.; Abbasi, B. H. Biogenic Synthesis and Characterization of Antimicrobial and Antiparasitic Zinc Oxide (ZnO) Nanoparticles Using Aqueous Extracts of the Himalayan Columbine (Aquilegia pubiflora). *Front. Mater.* **2020**, *7*, 249.
(73) Jan, H.; Khan, M. A.; Usman, H.; Shah, M.; Ansir, R.; Faisal, S.; Ullah, N.; Rahman, L. The Aquilegia pubiflora (Himalayan columbine) mediated synthesis of nanoceria for diverse biomedical applications. *RSC Adv.* **2020**, *10*, 19219−19231.
(74) Faisal, S.; Khan, M. A.; Jan, H.; Shah, S. A.; Abdullah, S.; Shah, S.; Rizwan, M.; Ullah, W.; Akbar, M. T.; Redaina, fnm Edible mushroom (Flammulina velutipes) as biosource for silver nanoparticles: from synthesis to diverse biomedical and environmental applications. *Nanotechnology* **2020**, *32*, 065101.
(75) Azza, Z.; Oudghiri, M. In vivo anti-inflammatory and antiarthritic activities of aqueous extracts from Thymelaea hirsuta. *Pharmacogn. Res.* **2015**, *7* (2), 213−216.
(76) Siddiqui, S. A.; Or Rashid, M. M.; Uddin, M. G.; Robel, F. N.; Hossain, M. S.; Haque, M. A.; Jakaria, M. Biological efficacy of zinc oxide nanoparticles against diabetes: a preliminary study conducted in mice. *Biosci. Rep.* **2020**, *40*, BSR20193972.
(77) Alkaladi, A.; Abdelazim, A.; Afifi, M. Antidiabetic activity of zinc oxide and silver nanoparticles on streptozotocin-induced diabetic rats. *Int. J. Mol. Sci.* **2014**, *15*, 2015−2023.
(78) Farag, M.; Al-Rehaily, A.; Ahmad, M. S.; Mothana, R. A. Detection of hypoglycemic and antidiabetic fraction in ethanol extract of Jatropha curcas aerial parts. *Pharmacol. Pharm.* **2014**, *05*, 663.
(79) Andrikopoulos, S.; Blair, A. R.; Deluca, N.; Fam, B. C.; Proietto, J. Evaluating the glucose tolerance test in mice. *Am. J. Physiol.: Endocrinol. Metab.* **2008**, *295*, E1323−E1332.
(80) Jan, H.; Shah, M.; Andleeb, A.; Faisal, S.; Khattak, A.; Rizwan, M.; Drouet, S.; Hano, C.; Abbasi, B. H. Plant-Based Synthesis of Zinc Oxide Nanoparticles (ZnO-NPs) Using Aqueous Leaf Extract of Aquilegia pubiflora: Their Antiproliferative Activity against HepG2 Cells Inducing Reactive Oxygen Species and Other In Vitro Properties. *BMC Complementary Med. Ther.* **2021**, *2021*, 1−14.

https://doi.org/10.1021/acsomega.1c05410
ACS Omega 2022, 7, 4071−4082